Proceedings of the 7th International Conference on Asian and Pacific Coasts (APAC 2013) Bali, Indonesia, September 24-26, 2013

NUMERICAL STUDY ON REGULAR WAVE OVERTOPPING FLOWS OVER SEA DIKE

X.Y. Guo [1], B.L. Wang [1,2] and H. Liu [1,2,3]

ABSTRACT: Based on the filtered Navier-Stokes equations and Smagorinsky turbulence model, a numerical wave flume is developed to investigate regular wave overtopping flow over trapezoidal smooth impermeable sea dike. Simulation of wave breaking is carried out to validate the numerical wave flume with wave generation and absorbing modules. With the in-house developed code, a series of test cases combined different crest heights and wave parameters are carried out. These results are compared with experimental results and numerical results available. The varying tendency of layer thickness and maximum velocity along dike crest is analyzed for both non-breaking and breaking regular waves. Then, the relationship between the magnitude of overtopping flow velocity and overtopping discharge is investigated.

Keywords: Filtered navier-stokes equations, regular wave overtopping flow, numerical wave flume, layer thickness, overtopping flow velocity, overtopping discharge.

INTRODUCTION

Due to the complicated hydrodynamic phenomena and engineering demanding, wave overtopping problem remains a hot research topic in these several decades. At the initial stage, the studies are mainly focused on the wave overtopping discharge and hydrodynamic forces by laboratory experiments and empirical formulas. A wave overtopping database including 10,000 tests is built up within the EU project CLASH as reported by van der Meer et al. (2009), which provides a wealth of data to researchers and a generic prediction method on mean wave overtopping discharge. Accompany with these valuable experimental data, numerical simulations has been proved to be a powerful tool to study overtopping in the recent decade. One kind of numerical model is based on nonlinear shallow water equations, e.g. Hu et al. (2000), Stansby and Feng (2004), Shiach et al. (2004), Ingram et al. (2009), Tuan and Ocumeraci (2010), which provide an efficient tools on evaluating the overtopping discharge. However, depth-integrated equations cannot be expected to accurately capture the wave breaking, turbulence transportation and significant vertical component of velocity. Meanwhile, another numerical models based on RANS model coupled with VOF method have been made great progresses and become a dominant numerical approach. Solving RANS model could provide a more comprehensive and detail description of wave overtopping process, especially for violent breaking waves, which are neglected in depth-integrate NLSW models. Some research have been carried out based on the RANS model such as Soliman(2003), Garcia et al. (2004), Lara et al. (2006), Reeve et al. (2008), Losada et al. (2008). Additionally, large-eddy simulation (LES) with a sub-grid scale (SGS) turbulence model is also investigated by Li et al. (2004), Park et al. (2008) and so on.

Although various numerical models have been studied for overtopping problems, detailed flow field studies are still in lack. For overtopping problem, Overtopping flow can cause the structure failure from the inner slope side of the sea-dike. The only knowledge of average overtopping rate is not enough to analyze structure functionality, stability and possible scour in the lee side. The velocity distribution is a crucial factor on evaluating the stability of the inner slope of the dike covered with green plants, clay or rubbles. However, the detail velocity distribution results is relative few and hard to measure especially for breaking waves in the laboratory. Schüttrumpf and Oumeraci (2005) investigated overflow velocities and thicknesses based on theoretical analysis and experimental validation. After Hurricane Katrina, horizontal velocity and overtopping flow thickness are experimentally studied for storm surge by Hughes and Nadal (2010). Peng and Zou (2011) investigated the spatial distribution of random wave overtopping using RANS-VOF model.

To fill in the gap between wealth overtopping data and velocity distributions, results achieved with various RANS and LES solvers can be used as an extension of the experimental overtopping discharge database.

[1] Department of Engineering Mechanics, Shanghai Jiao Tong University, Shanghai, CHINA
[2] Key Laboratory of Hydrodynamics of MOE, Shanghai Jiao Tong University, Shanghai, CHINA
[3] State Key Laboratory of Ocean Engineering, Shanghai Jiao Tong University, Shanghai, CHINA

Moreover, proper turbulent model and high resolution mesh enable the simulation running at the prototype scale, which illuminates a reliable use of the numerical simulations for engineering design.

The objective of the present work is to predict the maximum velocity and velocity distribution along the dike crest by the developed numerical model. Furthermore we attempt to find the relationship between the overtopping discharge and the maximum velocity based on numerical model results. Therefore we could estimate the velocity properties from the well-established empirical overtopping discharge formulations and the wave overtopping database.

MATHEMATICAL MODEL

Governing Equations

In present study, an immiscible, two dimensional incompressible and viscous two phase flows are considered. One set of equations is used to describe the behavior of the two phase fluids together, which includes the continuity equation and the filtered Navier-Stokes equations. These equations are:

$$\frac{\partial(\rho u_j)}{\partial x_j} = 0 \tag{1}$$

$$\frac{\partial(\rho u_i)}{\partial t} + \frac{\partial(\rho u_j u_i)}{\partial x_j} = -\frac{\partial}{\partial x_i}\left(p + \frac{2}{3}\mu\frac{\partial u_j}{\partial x_j}\right) + \frac{\partial}{\partial x_j}\left((\mu+\mu_t)\frac{\partial u_i}{\partial x_j}\right) + \frac{\partial}{\partial x_i}\left((\mu+3\mu_t)\frac{\partial u_j}{\partial x_j}\right) + \rho g_i \tag{2}$$

For two dimensional flow, x_i (i=1,2) represents two directions in Cartesian coordinate, t is the time, u_i is the filtered velocity components, ρ is the fluid density, μ_d and μ_t are molecular dynamic viscosity and turbulence viscosity respectively, g_i is the gravitational acceleration in the i-direction. According to the volume fraction function F, the density and viscosity of the mixture fluid can be expressed as general form:

$$f = Ff_w + (1-F)\, f_a \tag{3}$$

The subscripts w and a represent the variables of water and air respectively.

Turbulence Model

To estimate the small-scale turbulence generated during wave breaking, Smagorinsky turbulence model (Smagorinsky 1963) is employed which is widely applied in the flow simulations related to the free surface waves (Li et al. 2004 and Hieu et al. 2006). This model is closely connected to the strain rate and the grid size. The eddy viscosity μ_t is determined from the strain rate:

$$\mu_t = \rho(C_s\Delta)^2\sqrt{2S_{ij}S_{ij}} \tag{4}$$

Where Δ is a characteristic length scale of the small eddies depending on the mesh size and given by $\Delta = \min(\Delta x, \Delta y)$, C_s is Smagorinsky constant which is chosen as 0.075. $S_{ij} = \left(\partial u_i/\partial x_j + \partial u_j/\partial x_i\right)/2$

Two-phase Flow Model

The volume of fluid (VOF) algorithm is used to track the interface between air and water. For air-water flow, VOF method introduces function F to define water region. Function F is referred to as volume fraction of a cell occupied by water which can be evaluated as $F = V_W / V_C$, where V_w is the volume of water inside a cell and V_c is the cell volume. Hence, interface is established further:

$$F = \begin{cases} 0 & \text{in air} \\ 0 < F < 1 & \text{across the interface} \\ 1 & \text{in water} \end{cases} \tag{5}$$

The algorithm for tracking the free surface consists of two parts: interface reconstruction algorithm and interface advection algorithm. At each time step, the volume fraction function F is used to approximately reconstruct the interface with certain geometric solutions and the reconstructed interface is then used to evolve new volume fraction forward in time with solution of an advection equation. The two dimensional transport equation for F is given by:

$$\frac{\partial F}{\partial t} + \frac{\partial(Fu_j)}{\partial x_j} = F\frac{\partial u_j}{\partial x_j} \tag{6}$$

The algorithm for solving this equation follows the procedure of Pillod & Pucket (2004).

Method of solution

The governing equations are discretized by the finite volume method on staggered grids. Velocity components are evaluated at the cell sides, while scalar quantities are evaluated at the cell center. The convective terms in momentum equation are discretized by flux-limiter Van Leer scheme and the diffusion term is discretized with the central difference scheme. The Navier-Stokes equations are solved with the pressure correction procedure in form of the modified SIMPLE-type method. The resultant linear equation sets are solved using FGMRES iteration method (Saad 1993).

Numerical wave flume

Analytical relaxation approach is adopted for wave generation and absorbing in numerical wave flume. This method is originally presented by Mayer et al. (1998). Wang and Liu (2005) extended the analytical relaxation wavemaker approach and applied it to the numerical study of water wave based on the high order Boussinesq equations. In the past several years, the relaxation approach is formulated as an external force, i.e. source terms in the RANS equations, and implemented in commercial package Fluent with UDF. Some applications of the numerical wave flume on wave-structure interactions are investigated, such as Zhou et al. (2005), Liu et al. (2007).

Instead of using the source terms in the momentum equations, present study extends the original relaxation approach into the solution of the Navier-Stokes equations and implements wave generation and absorption by updating velocity directly at each time step, which can be expressed as:

$$\begin{aligned} u_M &= Cu_C + (1-C)u_I \\ v_M &= Cv_C + (1-C)v_I \end{aligned} \tag{7}$$

in which the velocity variables with the subscript C are the computed value from the Navier-Stokes solver, variables with subscript I denote the incoming wave velocity. $C = C(x)$ is the relaxation function related to spatial coordinate.

In general, the numerical wave flume is composed of four parts: wave maker zone, relaxation zone, work zone and sponger zone. In the wave maker zone, smoothly varying function C is assured that the velocities at right boundary are incoming wave velocity. At two ends of the wave maker zone, function C satisfies:

$$[C]_{x\min} = 1 \quad , \quad [C]_{x\max} = 0 \tag{8}$$

In the relaxation zone, function C is chosen for the purpose of eliminating the waves reflected from work zone. Function C satisfies:

$$[C]_{x\min} = 0 \quad , \quad [C]_{x\max} = 1 \tag{9}$$

In the sponger zone, function C is used to absorb the right-going waves out of work zone to prevent wave reflection at the boundary, which satisfies:

$$[C]_{x\min} = 1 , \quad [C]_{x\max} = 0 \tag{10}$$

Initial and Boundary Condition

At the initial time, still water is assumed in the whole computational domain and the pressure is given by the hydrostatic pressure. At the surface of solid structure, no-slip wall boundary condition is imposed by using one type of immerse boundary method, namely discrete forcing approach which is similar as what has been proposed by Mohd-Yusof (1997). The other kind of computational domain boundaries is symmetric boundary to satisfy no penetrating condition. The purpose of using no penetrating condition for bottom is to eliminate unnecessary viscous damping of wave energy during wave propagation along the work zone.

NUMERICAL VALIDATION

The validation of present numerical wave flume can be found in Guo et al. (2012). Here, wave breaking on a sloping bottom as the experimental conditions by Ting & Kirby (1994) is used for testing the numerical simulation of breaking waves on a sloping bottom. Fig.1 shows the bathymetry used in present computational model. Test wave is regular wave and the incident wave height H and period T in the constant water depth are 0.117m and 2s. According to the laboratory record, the breaking point is at x=6.4m where the local water depth is 0.197m, wave amplitude reaches 0.1625m due to shoaling effects on uneven bottom.

In the numerical wave tank, the computation domain is discretized using an orthogonal uniform grid with mesh size $\Delta x = \Delta y = 0.005$ for horizontal direction and vertical direction.

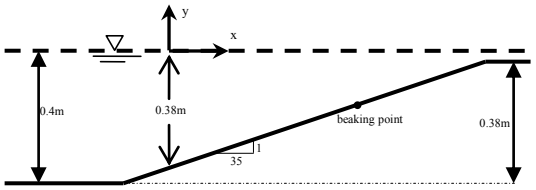

Fig. 1 Bathymetry in present computational model

Fig.2 shows the time histories of wave profile at breaking point x=6.4m. The surface elevations at different location are compared with experimental data (Ting and Kirby 1994) as illustrated in Fig.3. It can be seen that good agreement are obtained not only at breaking point but also before and after it. Fig.4 presents the comparisons of numerical results and experimental data for the phase averaged horizontal velocity components of different depth levels at different cross-section. It is observed from the figure that these velocities are well simulated.

It is indicated that present numerical model can reproduce with a high degree of agreement the free surface displacement, strong nonlinear shoaling on the

seaward slope, breaking point and velocity field after breaking.

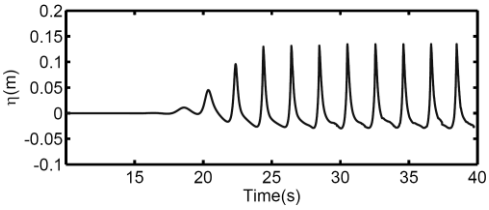

Fig. 2 time histories of wave profile at breaking point

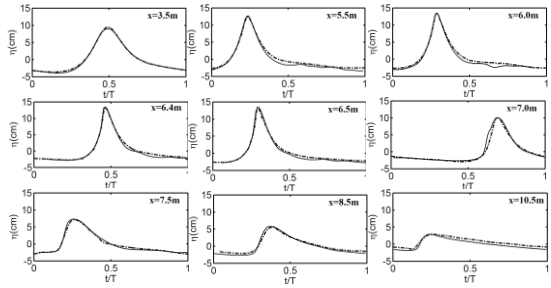

Fig. 3 Comparison of wave profiles at different locations, the solid line is the experimental data given by Ting & Kirby, the dash line is the present numerical results

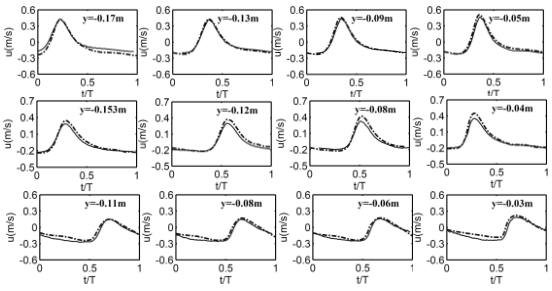

Fig. 4 Variation of phase-averaged horizontal velocity at different locations, the solid line is the experimental data given by Ting & Kirby(1994), the dash line is the present numerical results, from top to bottom: x=6.665m, x=7.275m, , x=8.495m.

Numerical Simulation of Overtopping over Sea dike

In this section, regular wave overtopping over seadike is investigated. The setup for the sea dike referred to Hu et al. (2000) is shown in Fig.5, $\cot\theta_s = 1.5$. Nine cases with different wave parameters and positive freeboard are simulated as illustrated in Table 1. The dimensionless overtopping rate Q was defined by Hu et al. (2000) as:

$$Q = \frac{q}{H_0\sqrt{gH_0}} \tag{11}$$

Where q is the dimensional average overtopping rates, g is the gravitational acceleration and H_0 is the deep sea wave height. q is statistically obtained by overtopping rates under steady state.

The standard deviation of overtopping rates is illustrated in Table 2 where the overtopping rates of present numerical results compared with the results from BWNM model by Soliman (2003), AMAZON model by Hu et al. (2000) and commercial software FLUENT. The experimental data used are derived by the small scale laboratory test data collected by Savile (1955). It can be seen from the table that present numerical model could predict overtopping discharge well.

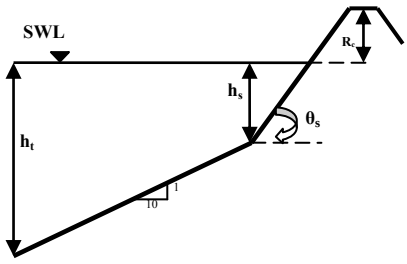

Fig. 5 Sketch of sloping seawall

Table 1 Configuration of simulated cases for regular wave simulation

No	h_t (m)	h_s (m)	R_c (m)	H_t (m)	T (s)	L_t (m)	H_0 (m)	L_0 (m)
1	3.0	1.5	0.5	0.95	4.73	23.8	1.0	34.9
2	3.0	1.5	1.0	0.95	4.73	23.8	1.0	34.9
3	4.0	1.5	0.5	1.08	7.98	49.2	1.0	99.3
4	4.0	1.5	1.0	1.08	7.98	49.2	1.0	99.3
5	4.0	1.5	1.5	1.08	7.98	49.2	1.0	99.3
6	6.0	2.0	0.67	1.2	12.8	98.2	1.0	255.6
7	6.0	2.0	1.33	1.2	12.8	98.2	1.0	255.6
8	6.0	2.0	2.0	1.2	12.8	98.2	1.0	255.6
9	6.0	2.0	2.67	1.2	12.8	98.2	1.0	255.6

Table 2 Standard deviation of overtopping discharges

	Amazon	2D BWNM	Fluent	Present study
σ	24.29	12.02	13.09	11.95

Table 3 test cases and corresponding overtopping rates

No	h_t (m)	R_c (m)	H_t (m)	T (s)	L_t (m)	H_0 (m)	L_0 (m)	Q (10^{-3})
10	4.0	0.5	0.92	4.0	21.1	1.0	25	55
11	4.0	1.0	0.92	4.0	21.1	1.0	25	29
12	4.0	1.5	0.92	4.0	21.1	1.0	25	10.4
13	4.0	0.5	0.97	6.0	35.3	1.0	56	73.2
14	4.0	1.0	0.97	6.0	35.3	1.0	56	39.6
15	4.0	1.5	0.97	6.0	35.3	1.0	56	19.9
16	4.0	0.5	1.4	6.0	35.8	1.4	56	70.8
17	4.0	1.0	1.4	6.0	35.8	1.4	56	38.2
18	4.0	1.5	1.4	6.0	35.8	1.4	56	27.7
19	6.0	0.67	0.93	6.0	41.0	1.0	56	75.4
20	6.0	1.33	0.93	6.0	41.0	1.0	56	31.6
21	6.0	2.0	0.93	6.0	41.0	1.0	56	9.5
22	6.0	2.67	0.93	6.0	41.0	1.0	56	0
23	6.0	0.67	1.04	9.0	66.3	1.0	126	92.1
24	6.0	1.33	1.04	9.0	66.3	1.0	126	42.9
25	6.0	2.0	1.04	9.0	66.3	1.0	126	14.5
26	6.0	2.67	1.04	9.0	66.3	1.0	126	3.4

In order to investigate overtopping flow on the crest dike in next section, another 14 cases simulated based on the same deep-sea wave heights as those in Table 1 and the overtopping rates shown in Table 3. Judging by the

formula for the critical wave height shown in Goda (1985), the waves for cases 10~18 have broken before overtopping.

INVESTIGATION OF OVERTOPPING FLOW ON CREST DIKE

A lot of seadike accidents manifest that overtopping flow is an important factor for the destruction of seawall. When seadike subjects to the serious overtopping, crest dike and landward dike will be under impacting and erosion and then lead to the damage or collapse of sea dike. Hence, overtopping flow on the crest dike should be assessed.

In this section, the distribution of layer thickness and overtopping flow velocity on the crest dike is studied based on the cases listed in table 3. Here, the definition of layer thickness is referred to as the maximum layer thickness at certain location (see Schuttrumpf and Oumeraci 2005) shown in Fig.6. The definition of overtopping flow velocity is similar with that of layer thickness. In the computation, the width of crest dike is 6m.

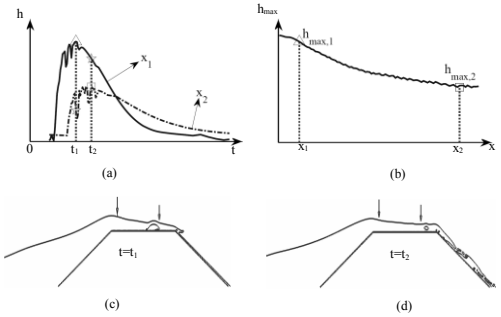

Fig.6 Definition sketch for maximum layer thickness: (a) Time histories of layer thickness at two typical locations x1(solid line) and x2(dashed-dot line), the maximum layer thicknesses are hmax,1 and hmax,2; (b) Distribution of maximum layer thickness along dike crest; (c) the free surface profile when the layer thickness is maximum at location x1; (d) the free surface profile when the layer thickness is maximum at location x2.

In Schuttrumpf & Oumeraci (2005), the expressions for layer thickness and maximum overtopping velocity are deduced based on boundary layer theory as equation (12) and equation (13).

$$\frac{h_C(x_C)}{h_C(x_C=0)} = \exp\left(-c\frac{x_C}{B}\right) \tag{12}$$

$$\frac{v_C(x_C)}{v_C(x_C=0)} = \exp\left(-\frac{x_C}{2}\frac{f}{h_C}\right) \tag{13}$$

Here, h_c is layer thickness on the dike crest, x_c is the coordinate on the dike crest with x_c=0 at the beginning and x_c = B at the end of the crest, B is the width of the dike crest, constant c is 0.75.

v is overtopping flow velocity on the dike crest, h=h_c is layer thickness, f is bottom friction coefficient, the value of f is 0.0058, v_0 = v_c (x_c=0) is overtopping velocity at the beginning of the dike crest.

Grid Convergence Study

Before the study of overtopping flow on crest dike systematically, grid convergence study is implemented using case 23. Different grid refinements with minimal grid size 0.1, 0.05 and 0.01 are used to compute layer thickness and overtopping velocity along crest dike. It can be seen from Fig.7 that the results are convergent as grid is refined. In the following study, the minimal grid size 0.01 is adopted.

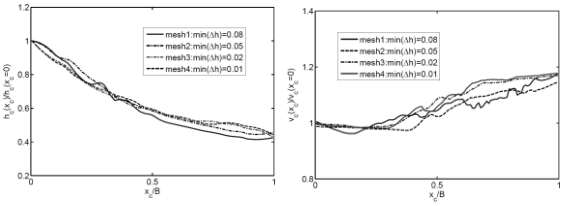

Fig.7 grid convergence study: layer thickness and flow velocity on the dike crest for case 23

Layer Thickness on Dike Crest

The layer thickness for different cases is shown in Fig.8 and compared with the analytical results in Schuttrumpf and Oumeraci (2005). It can be seen that present numerical results agree well with analytical results except for case 12 and case 15 which correspond to the small overtopping rates. It is indicated that the exponential decay law can describe the change of layer thickness on dike crest.

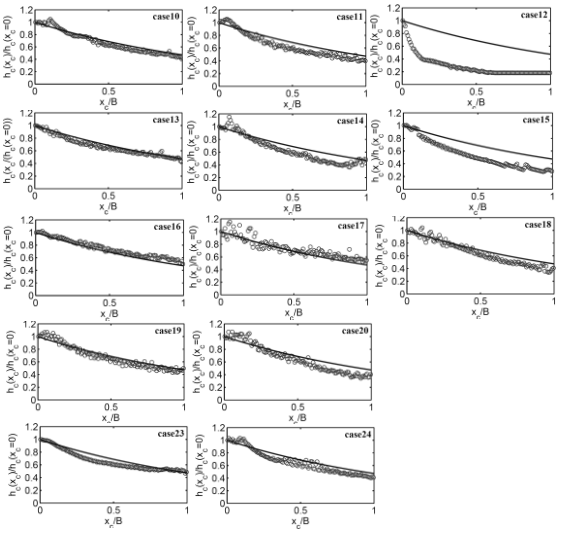

Fig.8 Distribution of maximum layer thickness along dike crest, the solid line is the theoretical results by Schüttrumpf and Oumeraci (2005), circle is the present numerical results.

Spatial Velocity Distribution on Dike Crest

Fig.9 shows the distribution of maximum velocity along dike crest for different cases. It is indicated that the numerical results have significant difference with the results calculated by formula (13). Maximum velocity increases along dike crest to some extent which doesn't obey the exponential decay law. Meanwhile, the results calculated by formula (13) using the computed layer thickness is given in Fig.9. These results are coincident with the analytical results which manifest that the formula (13) can't predict overtopping flow velocity under real complex free surface condition. In the local region near sea dike or on the crest dike, severe jet, splashing and air entrainment make the flow field much more complicated. Formula (13) is deduced based on the boundary layer theory which could confine its application.

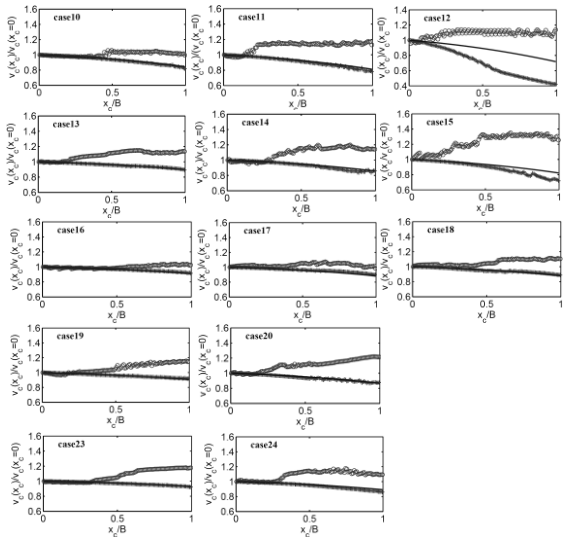

Fig.9 Distribution of maximum velocities along dike crest, the solid line is the theoretical results by Schüttrumpf and Oumeraci (2005), circle is the present numerical results, cross is the theoretical results based on the layer thickness computed by present model.

Correlation between Max Velocity and Overtopping Discharge

In present study, maximum velocities of certain locations on crest dike are monitored. The width of the crest dike 1m is used. M1 lies the front of the crest dike, M2, M3 and M4 are 0.1m, 0.5m and 1m from M1. According to the data recorded, the relationship between maximum horizontal velocity and overtopping rates is obtained by regression analysis in form of:

$$V_{\max}\Big/\sqrt{gH_0} = 0.362 + 1.40 * \tanh(0.0403Q) \qquad (14)$$

Fig.10 shows the fitted curves and the discretized values at M1, M2, M3 and M4. It can be observed from the figure: when overtopping rates is small, the maximum velocity is significantly affected by overtopping rates: the higher overtopping rates, the larger maximum horizontal velocity. When overtopping rates are at higher level, the effect of overtopping rates on the maximum velocity gradually reduced and becomes gentle.

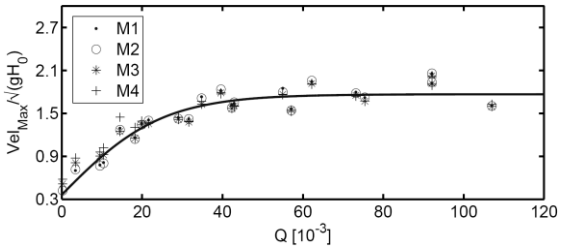

Fig.10 The relationship between maximum horizontal velocity and overtopping rates, the width of dike crest is 1m.

CONLUSION

A two dimensional numerical model is developed to study regular wave overtopping flow over trapezoidal smooth impermeable sea dike. Wave breaking in numerical wave flume is simulated to validate the capability of the model. It is found that the present model is efficient to simulate wave breaking. With the in-house developed code, systematic investigations on wave overtopping over trapezoidal smooth impermeable sea dike are implemented. A series of test cases combined different crest heights and wave parameters are carried out. These results are compared with experimental results and numerical results available. The varying tendency of layer thickness and maximum velocity along dike crest is analyzed for both non-breaking and breaking waves. It is indicated that layer thicknesses along dike crest decay at exponential rule, while maximum velocities along dike crest have an increasing tendency. Furthermore, the relationship between overtopping discharges and maximum horizontal velocities over the top of the dike is fitted tentatively.

The detailed analysis about velocity distribution and relationship between overtopping discharges and maximum horizontal velocities will be given in the future work.

ACKNOWLEDGEMENTS

The project was supported by the National Natural Science Foundation of China (Grant No. 10572093 and 11202129).

REFERENCES

Van der Meer, J.W., Verhaeghe, H., Steendam, G.J.(2009). The new wave overtopping database for coastal structures. Coast. Eng. 56: 108-120.

Hu, K., Mingham, C.G., Causon, D.M.(2000). Numerical simulation of wave overtopping of coastal structures using the non-linear shallow water equations. Coast. Eng. 41:433-465.

Stansby, P.K., Feng, T.(2004). Surf zone wave overtopping a trapezoidal structure: 1-D modeling and PIV comparison. Coast. Eng. 51:483-500.

Shiach, J.B., Minghan, C.G., Ingram, D.M., Bruce, T.(2004). The applicability of the shallow water equations for modeling violent wave overtopping. Coast. Eng. 51:1-15.

Ingram, D.M., Gao, F., Causon, D.M., Mingham, C.G., Torch, P.(2009). Numerical investigations of wave overtopping at coastal structures. Coast. Eng. 56:190-202.

Tuan, T.Q., Oumeraci, H.(2010). A numerical model of wave overtopping on seadikes. Coast. Eng.57: 757-772.

Soliman, A.S.M.(2003). Numerical study of irregular wave overtopping and overflow. Ph.D. Thesis, Univ. Nottingham, UK.

Garcia, N., Lara, J.L., Losada, I.J.(2004). 2-D numerical analysis of near-field flow at low-crested permeable breakwaters. Coast. Eng.51: 991-1020.

Lara, J.L., Garcia, N., Losada, I.J.(2006). RANS modeling applied to random wave interaction with submerged permeable structures. Coast. Eng.53: 395-417.

Reeve, D.E., Soliman, A., Lin, P.Z.(2008). Numerical study of combined overflow and wave overtopping over a smooth impermeable seawall. Coast. Eng.55:155-166.

Losada, I.J., Lara, J.L., Guanche, R., Gonzalez-Ondian, J.M.(2008). Numerical analysis of wave overtopping of rubble mound breakwaters. Coast. Eng.55:47-62.

Li, T.Q., Troch, P., De Rouck, J.(2004). Wave overtopping over a sea dike. J. Comput. Phys. 198:686-726.

Park, J.C., Lee, B.H., Hong, K.Y.(2008). Wave overtopping simulations over coastal structures. J. Mech. Sci. Tech. 22:1222-1229.

Schüttrumpf, H., Oumeraci, H.(2005). Layer thicknesses and velocities of wave overtopping flow at seadikes. Coast. Eng.52:473-495.

Hughes, S. and Nadal, N.(2009). Laboratory study of combined wave overtopping and storm surge overflow of a levee. Coast. Eng.56:244-259.

Peng, Z., Zou, Q.P.(2011). Spatial distribution of wave overtopping water behind coastal structures. Coast. Eng. 58:489-498.

Smagorinsky, J.(1963). General circulation experiments with primitive equations: I. The basic experiment. Monthly Weather Review, 91: 99 ~ 164.

Hieu, P.D., Tanimoto, K.(2006). Verification of a VOF-based two-phase flow model for wave breaking and wave-structure interactions. Ocean Eng. 33:1565-1588.

Pilliod, J.E., Puckett, E.G.(2004). Second-order accurate volume-of-fluid algorithms for tracking material interfaces. J. Compt Phys.199: 465–502.

Saad, Y.(1993). A flexible inner-outer preconditioned GMRES algorithm. SIAM Journal on Scientific and Computing, 14: 461-469.

Mayer, S., Garapon A., Sorensen L.S.(1998). A fractional step method for unsteady free-surface flow with applications to nonlinear wave dynamics. Int. J. Numer. Meth. Fluids. 28:293-315.

Wang, B.L., Liu, H.(2005). Higher order Boussinesq-type equations for water waves on uneven bottom. Appl. Math. Mech.26(6): 714 ~ 722. (in Chinese)

Zhou, Q.J., Wang, B.L., Lan, Y.M., Liu, H.(2005). Wave overtopping simulation in a Fluent numerical wave flume. Chinese Quarterly of Mechanics,36(4): 629 ~ 633. (in Chinese)

Liu, Y.N., Guo, X.Y., Wang, B.L., Liu, H.(2007). Numerical simulation of wave overtopping over seawalls using the RANS equations. J. Hydrodyn. Ser. B. 22(6): 682 ~ 688. (in Chinese)

Mohd-Yusof, J.(1997) Combined immersed-boundary/B-spline methods for simulations of flow in complex geometries. Technical report, Center for Turbulence Research.

Guo, X., Wang, B., Liu, H.(2012). Numeircal simulation of irregular wave overtopping against a smooth sea dike. China Ocean Eng. 26(1): 153-166.

Ting, F.C.K., Kirby, J.T.(1994) Observation of undertow and turbulence in a laboratory surf zone. Coast. Eng. 24:51-80.

Saville, T.(1955). Laboratory data on wave runup and overtopping on shore structures. Dayton, Ohio, U.S.Army, Beach Erosion Board, Document Service Centre, No. 64.

Goda, Y.(1985) Random seas and design of maritime structure. University of Tokyo Press.